15TH IEA HEAT PUMP CONFERENCE
MAY 26–29, 2026 | HOFBURG VIENNA 2026
DECARBONISATION THROUGH INNOVATION

Experimental demonstration of an ammonia-salt resorption cycle heat pump

R.E. Critoph[a*], G.H. Atkinson[a], S.J. Metcalf[a], G.S.F. Shire[a]

[a] School of Engineering, University of Warwick, Coventry CV4 7AL, UK

Abstract

The design, manufacture, test and analysis of a kW-scale proof-of-concept resorption heat pump is presented. The adsorbent reactors use sodium bromide and manganese chloride salts with ammonia refrigerant. The reactor design was informed by Large Temperature Jump (LTJ) testing using a representative 'unit-cell' reactor. Extensive LTJ tests were conducted on ammonium chloride and sodium bromide, the latter being chosen as a suitable low temperature salt. Manganese chloride was selected as the high temperature salt. The salt selection methodology and analytical tools used in the LTJ analysis have been advanced compared with previous works, providing greater confidence in the identification of suitable salts and the working 'equilibrium' lines.

The design of the heat pump is summarised, detailing component selection, calibration, and measurement and control methodologies. Compact adsorption reactors and a supporting test rig to measure and assess reactor performance are described.

Automatic resorption cycling control has been achieved, enabling over 100 resorption cycles to be completed with continually connected reactors. Ammonia mass flow measurements and reactor heat transfer fluid heat balances show consistent, repeatable cycling and from which, dynamically measured COPs and power outputs were calculated taking into account all thermal masses.

The contact resistance between the composite salt and the tube is limiting, resulting in a lower than designed power output. Swelling of the salt composite has also been observed, however, there is no evidence of performance degradation.

COPs in the range 1.04 up to 1.28 have been achieved with average power outputs in the range 750 W to 3 kW (490 and 690 W/kg salt or 60 to 85 W/litre). Analysis of the dynamic performance and optimum control strategies are discussed.

As designed, the resorption system is for domestic heating, but more widely the results show promise for use of ammonia-salt reactions for use in recoverable (waste) heat upgrading.

Selection and/or peer-review under the responsibility of the organizers of the 15th IEA Heat Pump Conference 2026.

Keywords: Chemisorption; heat pump; ammonia

1. Introduction

Heating and cooling of buildings (residential and industrial) contributes significantly to global warming through the release of carbon dioxide (CO_2) emissions. A recent report indicates that "*nearly 40 % of energy-related CO_2 emissions*" are attributed to heat, and only half of the additional annual heat demand (+7 %, 2017-2023) has been satisfied by renewable heat [1]. One specific area of interest in providing clean, or cleaner, heat, are sorption systems. Sorption systems have long been of interest. The use of lower carbon fuels, the advancement of efficient and novel thermal technologies are all important in achieving national and global emissions targets. Sorption systems are an alternative thermal energy technology and have the potential to be used in thermal storage, refrigeration, heat pump and heat transformation applications.

* Corresponding author. Tel.: +44 7973814888
E-mail address: R.E.Critoph@warwick.ac.uk

Sorption systems are classified as 'absorption' relying on the absorption of a refrigerant into a liquid absorbent, 'adsorption' relying on the adsorption of a refrigerant into a solid (generally by means of van der Waals forces, or 'physisorption') or 'chemisorption' relying on the adsorption of a refrigerant into a solid by means of a reversible chemical reaction. This research is on a chemisorption heat pump using a resorption cycle with two different sorbents.

1.1. Resorption Cycles

In a resorption chemisorption cycle the refrigerant is cycled back and forth between two different chemical salts to achieve (in our case) heat pumping. This has the advantage that the enthalpies of sorption are generally much higher than the latent heat of the refrigerant, leading to higher COPs. Also there is no need for an evaporator, condenser or expansion device, potentially reducing complexity and manufacturing costs.

Figures 1(a) and 1(b) show a block diagram of the essential components in the two operating phases and Figure 1(c) the Clapeyron diagram of the basic cycle.

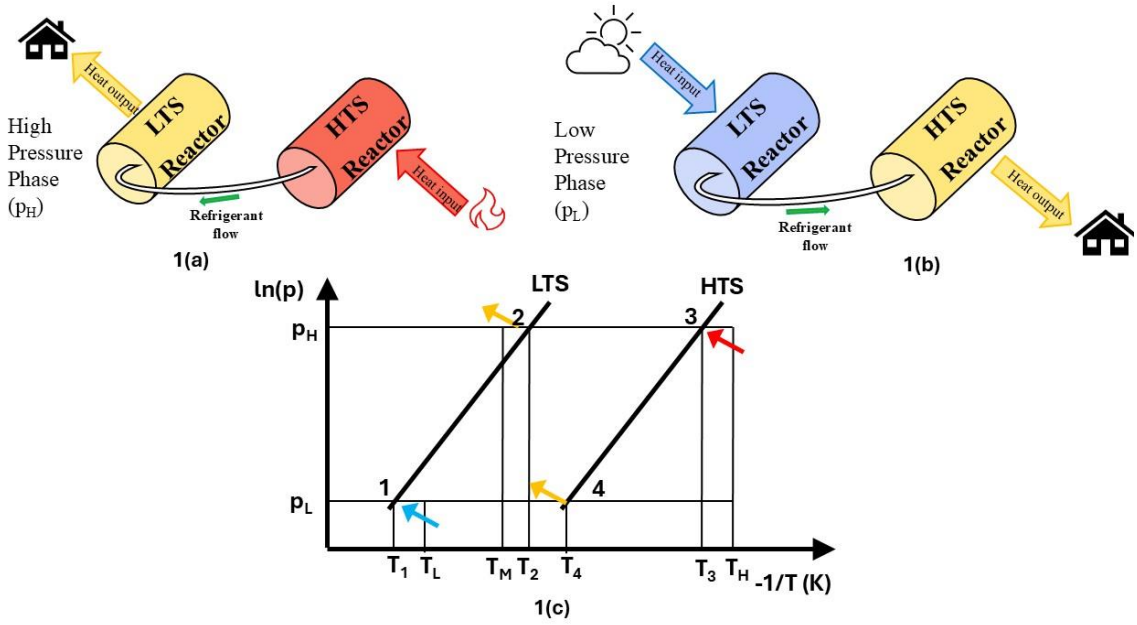

Figure 1. Reactors in high pressure phase (a), reactors in low pressure phase (b) and Clapeyron diagram (c)

One reactor contains a Low Temperature Salt (LTS) and the other a High Temperature Salt (HTS). The equilibrium lines for adsorption and desorption, assuming no hysteresis, are shown by the bold lines in Figure 1c. The idealized cycle consists of a high-pressure phase (Figure 1a) a low-pressure phase (Figure 1b) and pressurisation and depressurisation processes.

In the high-pressure phase (HPP), high grade heat (e.g. from a combustion process) at temperature T_H heats the HTS, desorbing refrigerant at T_3 , corresponding to point 3 in Figure 1c. The refrigerant is adsorbed in the LTS, generating heat at T_2, point 2 in Figure 1c. This is part of the heat output of the heat pump, removed by a fluid at T_M. When the reaction is deemed to have progressed sufficiently towards completion (this is a control parameter) the HTS is cooled by the fluid at T_M and the LTS is thermally isolated, with no fluid flow. This has the effect of depressurizing the system from p_h to p_l . The state of the HTS moves from point 3 to point 4 and that of the LTS from point 2 to point 1. There is a small transfer of refrigerant from the LTS to the HTS resulting in the drop of temperature of the LTS.

At this point the low-pressure phase (LPP) commences, as shown in Figure 1b. Ambient heat at T_L is transferred to the LTS, desorbing refrigerant at T_1. The refrigerant is adsorbed in the HTS, generating heat at T_4 which is removed by the fluid at T_M forming the second part of the useful heat output. The cycle is completed by a pressurisation process in which the LTS is adiabatic with no fluid low through the reactor and the HTS is heated from T_4 to T_3 using heat from the fluid at T_H. There is a small transfer of refrigerant from the HTS to the LTS resulting in the final temperature of the LTS reaching T_2.

Higher efficiency versions of the resorption cycle are possible. They include recovery of heat between the pressurization and depressurization processes.

1.2. Choice of salts and refrigerant

Refrigerants used in sorption cycles benefit from having high latent heat, and the practical options are water, ammonia and alcohols. Given the benefits afforded by operating at above atmospheric pressure we have chosen to use ammonia. There are a wide range of salts available that form ammoniates, with a wide range of equilibrium conditions, allowing a suitable pair to be selected for most applications. Ammonia-halide salt cycles have been investigated since the 1980s; a detailed review is given in [2] and particular mention made of the work carried out by Spinner, Neveu, Stitou and others from the Institute of Science and Engineering of Materials and Processes (CNRS PROMES) at the University of Perpignan [3,4,5].

The LTS used was sodium bromide (NaBr) and HTS was manganese chloride ($MnCl_2$). The detailed selection is justified in [6], but the essential constraints are to avoid low pressures that might result in poor mass transfer, and for -10 °C <T_L<10° C, 50 °C <T_M<70 °C and 170 °C <T_H<200 °C. The chemical reactions are as in Eq. (1 and 2):

$$NaBr + 5.25NH_3 = NaBr \cdot 5.25NH_3 + Q_{0-5.25} \quad (1)$$

$$MnCl_2 \cdot 2NH_3 + 4NH_3 = MnCl_2 \cdot 6NH_3 + Q_{2-6} \quad (2)$$

where $Q_{\#-\#}$ is the heat of reaction. If the reaction is reversible (no hysteresis) then the relationship between equilibrium temperature and pressure of a reaction is given by Eq, (3):

$$ln\, p = \frac{-\Delta H}{R_0 T} + \frac{\Delta S}{R_0} \quad (3)$$

where p = pressure (Pa), ΔH = reaction enthalpy change (J mol^{-1}), ΔS = reaction entropy change (J mol^{-1} K^{-1}), R_o = universal gas constant (J mol^{-1} K^{-1}) and T = temperature (K) which, when plotted on an axis of ln(p) versus -1/T, is known as a Clapeyron diagram (with the slope of the line equal to ΔH / R_o and the intercept equal to ΔS / R_o. However, if there is hysteresis, and the reaction is not reversible the reaction enthalpy will no longer be given by the slope of the line. Where hysteresis is present, the heats of adsorption and desorption must be nearly identical as discussed in [7] and as in Eq. (4):

$$\Delta H_{ads} - \Delta H_{des} = \Delta T_{HYS}(c_{v\,ADS} - c_{v\,GAS}) \quad (4)$$

where ΔH_{ads} is the heat of adsorption (J mol^{-1}), ΔH_{des} is the heat of desorption (J mol^{-1}), ΔT_{HYS} is the temperature difference between adsorption and desorption at the same pressure (K), $c_{v\,ADS}$ is the specific heat of the adsorbed phase (J mol^{-1} K^{-1}) and $c_{v\,GAS}$ is the specific heat of the gas phase (J mol^{-1} K^{-1}). Experimental valuation of the sorption heats and equilibrium lines is described in section 3.1.

2. Design of reactors and experimental rig

2.1. Reactor design and construction

The acknowledged challenges of chemisorption in salts are firstly to get adequate heat and mass transfer and secondly to cope with the excessive swelling of the salts, which can lead to agglomeration and degradation of performance over time. We impregnate the salts into an Expanded Natural Graphite (ENG) matrix to address both these problems. The ENG is commercially available SIGRATHERM board, density 150 kg m^{-3} and 10 mm thick. Experiments on small quantities of this composite are reported in [7,8,9].

The reactor design is based around a unit cell of ENG as shown in Fig. 2. The ENG hexagon is 32 mm across the flats with a central 12.7 mm hole to take a tightly fitting stainless steel tube that contains the heat transfer fluid (HTF); pressurised water. The water to tube heat transfer is enhanced by CALGAVIN hiTRAN tube inserts.

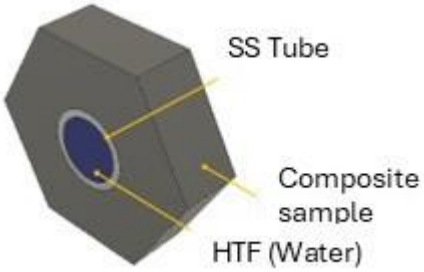

Figure 2. Unit cell of ENG composite

A number of these (50 for the HTS reactor, 66 for the LTS reactor) are fitted onto the stainless steel tube and seven such tubes are combined in a shell to form each reactor as shown in Fig. 3.

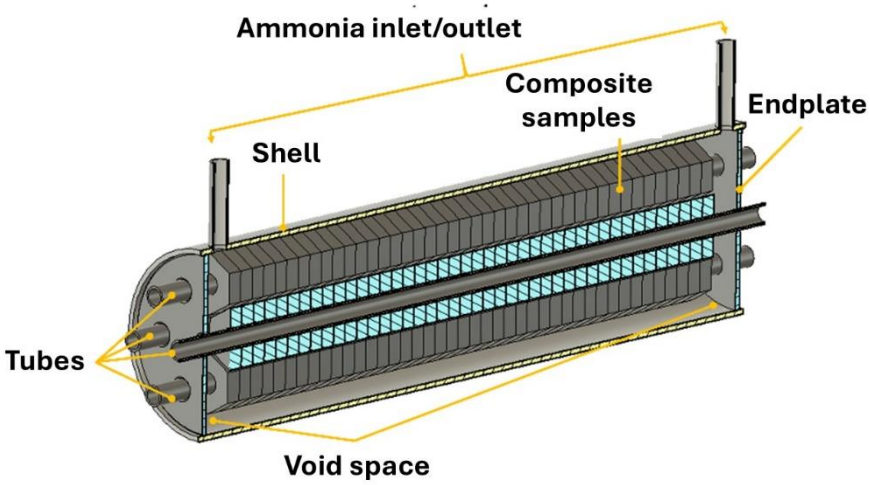

Figure 3. Reactor design

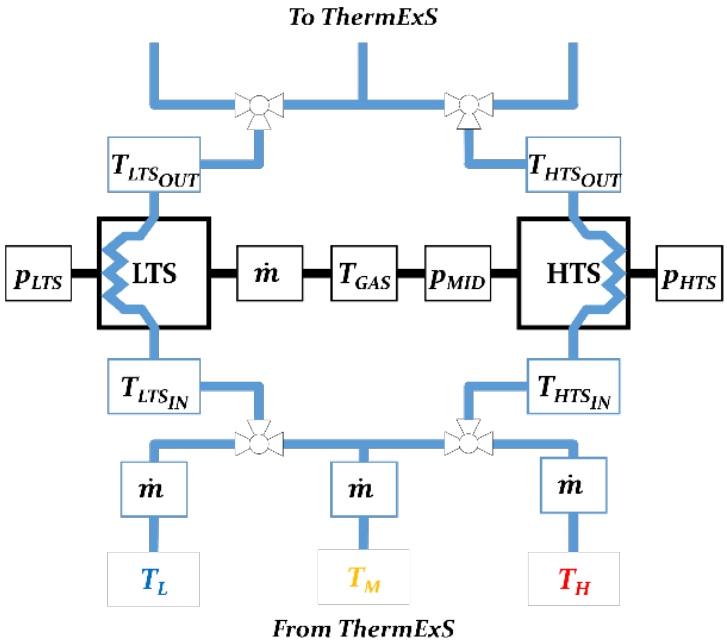

Figure 4. Block diagram of HTF and ammonia system showing instrumentation points (pressure p , temperature T, mass flow rate $\dot{m}$)

2.2. Experimental rig

A block diagram of the whole system in Fig. 4 and a photograph in Fig. 5. The pressurised water HTF at temperatures T_L, T_M and T_H is supplied from the 'ThermExS' test stand which has three thermostatically controlled heaters having the required temperature range and flows.

2.3. Instrumentation and control

Water and ammonia mass flow rates were all measured by Micro Motion Elite Coriolis mass flow meters with an accuracy of +/- 0.25 % of flow. Temperatures were measured by Class A PT100 sensors and matched pairs were used to measure inlet and outlet water temperatures so that the error contributing to heat flow measurements and under calibration all sensors maintained an overall spread of no more than 0.1 °C and an uncertainty of ±0.05 °C. Pressure was measured by Danfoss AKS32 pressure transducers which were calibrated in a dead weight tester. Combining the errors to calculate the accuracy of the power to/from the reactors, suggests a maximum error of 46 W. Against the target power output of 2.5 kW, this is in the region of 2 %, or 4 % of the power actually achieved. Data acquisition and control of all pumps, valves and the ThermExS heaters/coolers was via an NI cDAQ connected to a laptop running a LabView program.

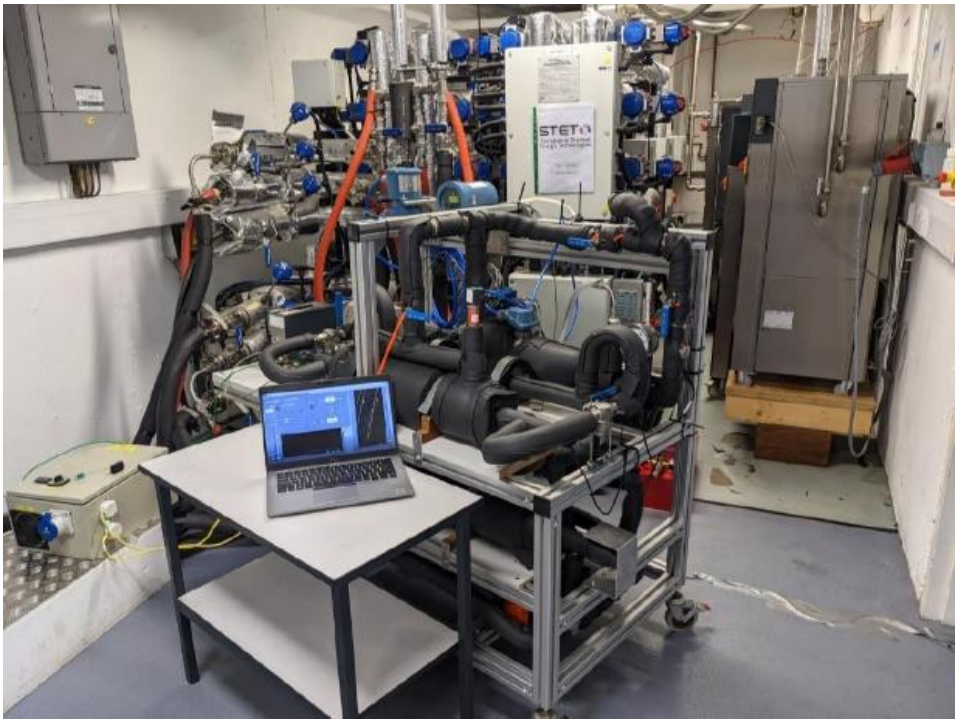

Figure 5. Image of the proof-of-concept resorption experimental rig in front of the ThermExS test facility

3. Results

3.1. Salt equilibrium lines and hysteresis

The equilibrium lines were directly measured in the test rig and compared with other reported data. It is well known that the quantity of hysteresis observed can vary depending on the scale and the experimental apparatus used. Each reactor could be isolated and a series of p, T points measured by stepping the temperature up to a maximum and then down again. The set temperature was raised, then lowered in 10 ° C steps, each step taking 1000 s. The final 300 s of data in each step was unchanging and assumed to be in equilibrium.

The NaBr (LTS) reactor results are in Fig. 6, where they are compared with previous data measured in a Large Temperature Jump apparatus [6]. It is noticeable that our results suffered no hysteresis whereas the previous study implied a temperature difference of around 5 °C. Our results are denoted by the circled points and the previous results by lines.

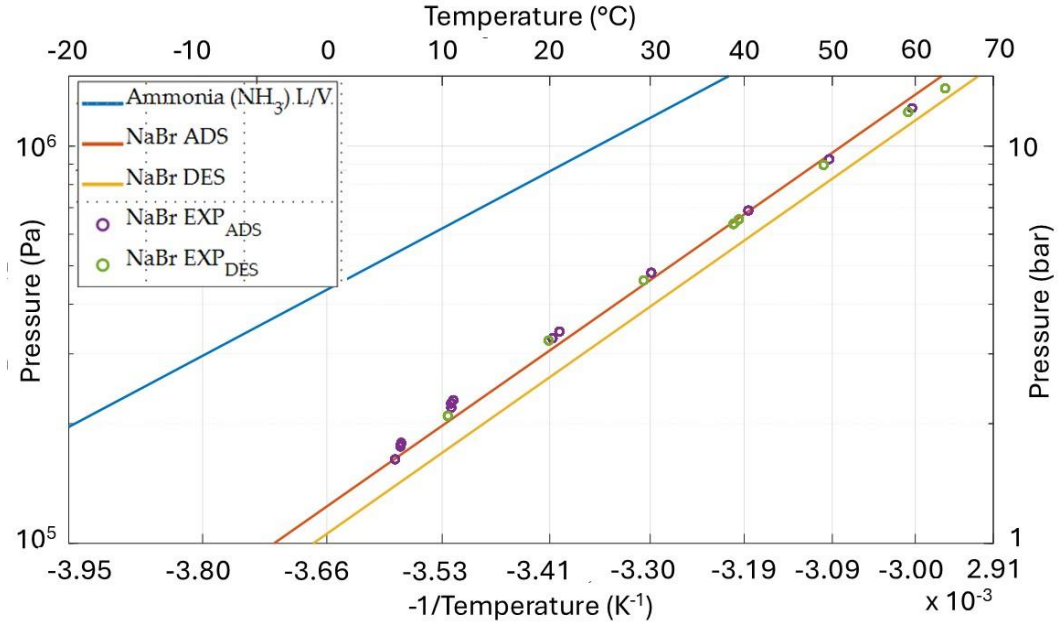

Figure 6. Equilibrium lines of the ammonia-NaBr reaction

Similar results for the $MnCl_2$ (HTS) reactor are in Fig. 7 and compared with [7]. Again, the behaviour in our apparatus shows almost no hysteresis. Our results are almost identical to Neveu and Castaing [3] who reported no hysteresis.

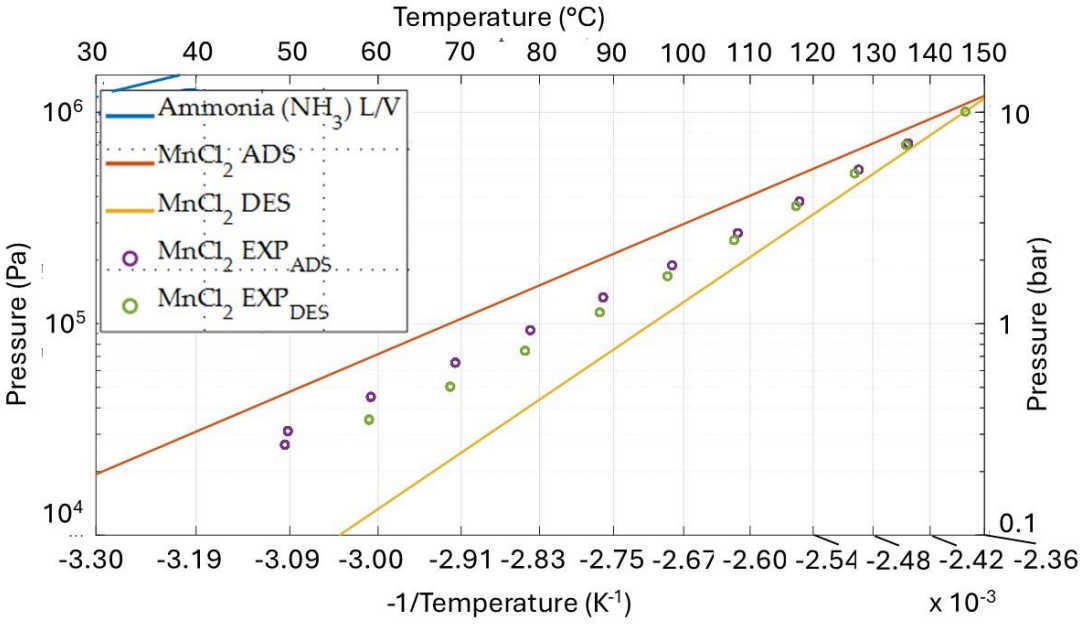

Figure 7. Equilibrium lines of the ammonia-$MnCl_2$ reaction

The equilibrium lines established are important, both to help analyse cyclic testing results and more generally. It is particularly notable that there is little or no hysteresis occurring in this kW scale machine compared with tests on smaller quantities of salts by ourselves and other authors using similar times to reach equilibrium, and this needs further investigation.

3.2. Full length cycles

When operating, the duration of the cycle phases is controlled out automatically by the LabView program and interfaces that switch water valves and turn water pumps on and off. Results are very repeatable, and on changing conditions, a new steady cycle is evident from the fourth cycle after the change. More than 100 cycles have been carried out and there is no measurable degradation of performance. The raw data measured consists of the water inlet and outlet temperatures of both reactors, the water flow rate, the ammonia flow rate, and pressures in both reactors and their connection. In cycling tests all three pressures are identical, pressure drops being negligible. The HTS and LTS adsorbent temperatures are not directly measured, and a single temperature would not be overly useful since temperature varies throughout the reactor. Only when carrying out the equilibrium tests is there a single reactor temperature and it is identical the temperature of the water flowing through the reactor. In later analysis, although a simplification, the representative temperature of the salt is taken as the mean temperature of the water flowing through the reactor.

A typical set of raw data for five cycles is given in Fig. 8. Ammonia mass flow is taken as positive in the LPP and negative in the HPP.

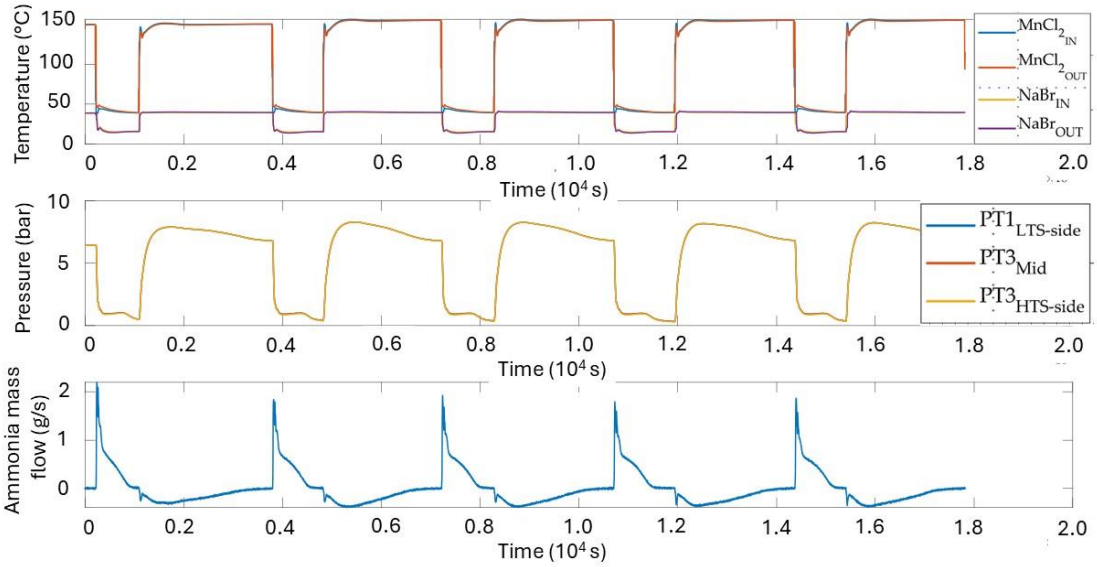

Figure 8. Typical raw data recorded over five steady cycles.

Note that the phases are not of equal duration. The LPP has greater driving temperature differences and is shorter. The HPP takes two times longer to reach completion. There are alternative approaches of interpretation of the physics. Goetz, Elie and Spinner [10] and Bao, Zhiwei and Roskilly [11] consider the chemical reaction rate to be limiting and the driving force to be related to the difference between the temperature of the salt and the equilibrium temperature at the prevailing pressure. Hinmers et al. [7] analysed LTJ results of samples similar to those used here and concluded that the reactions were dominated by heat transfer rather than chemical non-equilibrium. Fig.9 shows the temperature differences between the assumed salt temperature (actually the mean water temperature) and the equilibrium temperature (derived from the pressure). Whether this is demonstrating a heat transfer or chemical reaction limit, it is clear that the LPP has a higher driving potential, with the LTS having only around 5 °C in the HPP compared to 15 °C in the LPP.

The mass flow of ammonia, a direct measure of reaction advancement is shown in Fig. 10. The differences between the HPP and LPP are clear. Integration of the mass flows reveals the advancement of the reactions during the cycle. Fig. 12 shows that the HTS cycles 95 % of the ammonia theoretically possible, whilst the LTS only cycles 75 %. This was despite best efforts to ensure the reactors had ‘balanced’ masses of salt within

them: 0.63 kg NaBr and 0.86 kg $MnCl_2$. However, not all the salt crystals are accessible, and it is difficult to control for this.

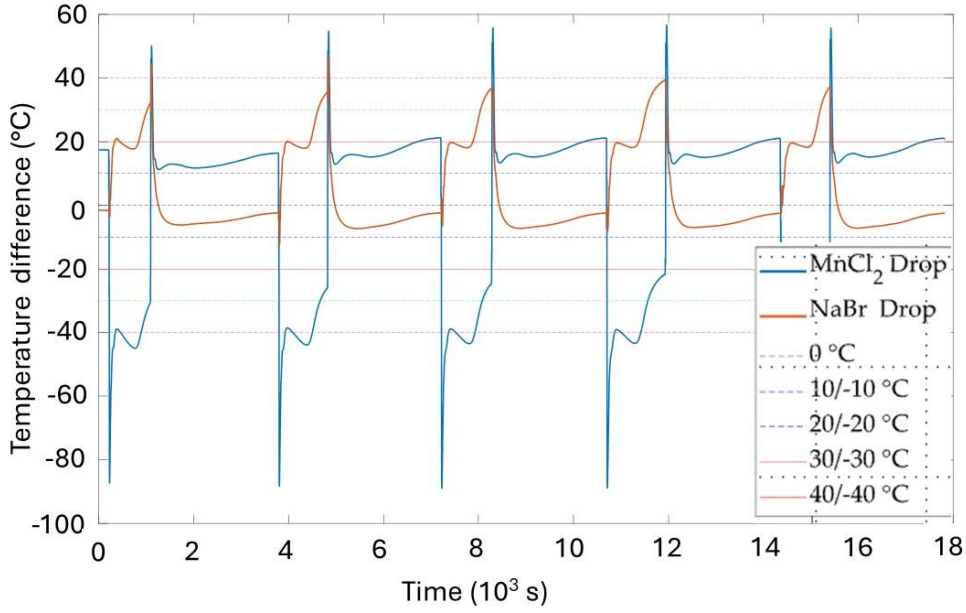

Figure 9. Driving temperature differences

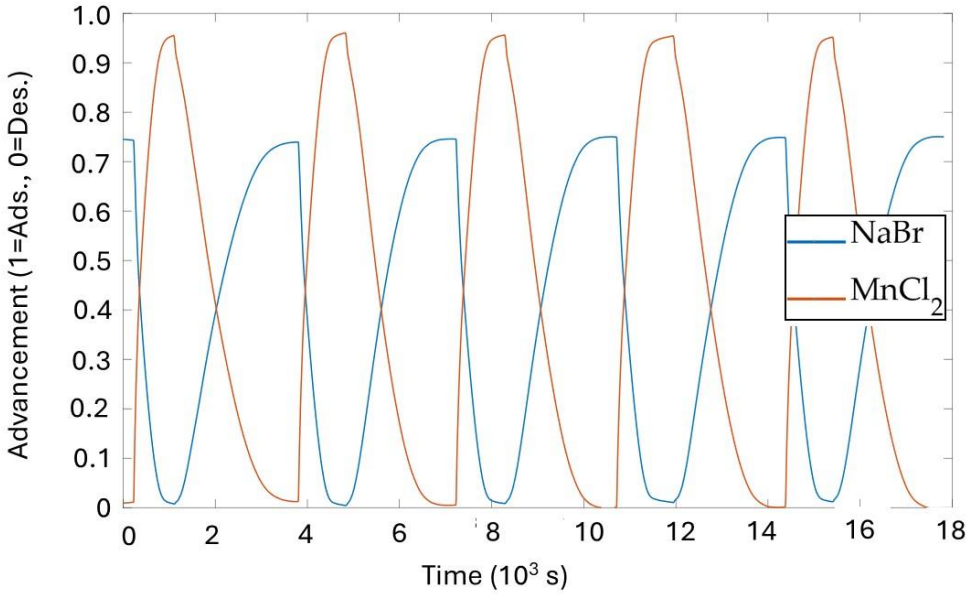

Figure 10. Reaction advancement in each reactor

COPs and mean power output were calculated for four different test conditions, as shown in Table 1. For comparison, a theoretical cycle operating with T1 = 0 °C, T2 = 40 °C, T3=132 °C, taking thermal masses into account would have a COP of 1.35. The differences mainly arise from heat leakages into the reactor shells with subsequent thermal cycling and mis-matched accessible salt masses. The designed power was up to 2.5 kW, twice the experimental value. The cause is probably the worse than expected fit of the hexagonal ENG elements onto the tubes. The LTJ tests that provided the design thermal contact coefficient used a small number of carefully fitted elements and it is likely that the many hundreds used in the test rig could not maintain their

tight fit during assembly. The simulation model used in analysis of the LTJ tests [7] showed that the power achieved is very sensitive to the contact resistance, and a poorer fit in the generators than assumed could well account for the lack of power.

Table 1. Full cycle test results of power and COP

Setpoint Temperatures (Delivered) / °C			No. of Cycles	Cycle Time / (s)*			Average Power / W	COP
T_H	T_M	T_L		LPP	HPP	Total		
160 (155)	40 (40)	15 (15)	5	1000	2400	3400	749	1.274
170 (165)	40 (40)	15 (15)	5	1000	1600	2600	996	1.268
175 (170)	40 (40)	15 (15)	5	1000	1500	2500	1036	1.258
175 (170)	40 (40)	15 (15)	7	1000	1600	2600	1024	1.245

3.3 Shorter length cycles

In a practical heat pump, it is probable that two sets of reactors would be run out of phase. This would allow the high grade heat input and low grade (ambient) input to run continuously and without storage. This requires the duration of the LPP and HPP to be equal, which reduces the quantity of ammonia transferred and hence the COP. However, there is a benefit in terms of increased mean power. A number of cycles were run with reduced cycle times to explore the tradeoff. The temperature conditions chosen were T_H=160 °C, T_M=40 °C, T_L=15 °C and the half-cycle times varied from 1300s to 60s. The corresponding COPs and mean power output are shown in Fig. 11.

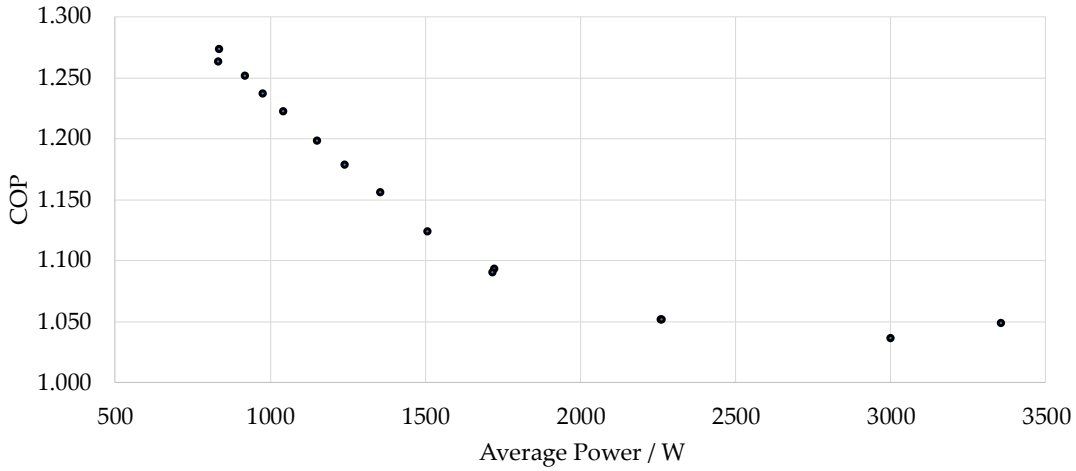

Figure 11. COP v. Power output for a range of equal length half-cycles

The trend of increasing power with decreasing COP as the cycle time is reduced is clear. The COP plateaus as the power continues to increase. This highlights the rapid recovery of sensible heat during short cycling, rather than a useful heat pumping output.

4. Conclusions

Overall, the results demonstrate that the proof-of-concept resorption test rig has operated successfully, with a minimal complexity resorption cycle. The analysis of the cycles provides previously unreported detail and

insight regarding the continual nature of coupled chemical adsorption reactions, which will be valuable in future research. In all, over 100 cycles have been completed using automatic cycling with continually coupled reactors, a first for a NaBr - $MnCl_2$ resorption pairing for potential application in a domestic gas fired resorption heat pump.

The results have not achieved the desired 1 kW/kg_{SALT} goal or the predicted COP of about 1.35. The power deficit is due to the thermal contact resistance between the composite salt and the heat transfer tube interface. The reduced COP is due to the thermal mass of the reactors and the mis-matched ratios of the two salts that are accessible to ammonia within the reactors. All these issues may be addressed in a second design iteration. The COPs reported (1.04-1.25) are comparable to prior works by Vasiliev et al. [12] and Blackman, Bales and Thorin [13]. Low power outputs (750-3000 W) are disappointing, but on a mass (490-690 W/kg_{SALT}) and volume (60-85 W/litre) specific basis, the results show the best specific power performance reported on a resorption heat pump system to date.

Acknowledgements

The research was supported by:

- EPSRC Standard Research Grant (EP/V011316/1) – Sorption Heat Pump Systems;
- EPSRC Programme Grant (EP/R045496/1) – LoT-NET; and
- EPSRC DTP Studentship (EP/R513374/1 (2199243)) – Doctoral Studentship.

References

[1] International Energy Agency (IEA), "Renewables 2024," Paris, France, 2024. [Online]. Available: https://www.iea.org/reports/renewables-2024

[2] G. H. Atkinson and R. E. Critoph, "A review of experimental works using ammonia-salt adsorption reactions," International Journal of Refrigeration, 2025, doi: 10.1016/j.ijrefrig.2025.04.024..

[3] P. Neveu and J. Castaing, "Solid-gas chemical heat pumps: Field of application and performance of the internal heat of reaction recovery process," Heat Recovery Systems & CHP, vol. 13, no. 3, pp. 233-251, 1993.

[4] FN. Mazet, M. Amouroux, and B. Spinner, "Analysis and experimental study of the transformation of a non-isothermal solid/gas reacting medium," Chemical Engineering Communications, vol. 99, no. 1, pp. 155-174, 1991, doi: 10.1080/00986449108911585.

[5] E. Lepinasse, V. Goetz, and G. Crozat, "Modelling and experimental invetigation of a new type of thermochemical transformer based on the coupling of two solid-gas reactions," Chemical Engineering and processing: Process Intensification, vol. 33, pp. 125-134, 1994, doi: 10.1016/0255-2701(94)90002-7.

[6] G. H. Atkinson, S. J. Metcalf, R. E. Critoph, G. S. F. Shire, and M. van der Pal, "Design and manufacture of a proof-of-concept resorption heat pump using ammonia-salt chemisorption reactions," Cleaner Energy Systems, vol. 6, p. 100082, 2023, doi: 10.1016/j.cles.2023.100082.

[7] S. Hinmers, G. H. Atkinson, R. E. Critoph, and M. van der Pal, "Modelling and Analysis of Ammonia Sorption Reactions in Halide Salts," International Journal of Refrigeration, 2022, doi: 10.1016/j.ijrefrig.2022.01.032

[8] S. Hinmers and R. E. Critoph, "Modelling the ammoniation of barium chloride for chemical heat transformations," *Energies,* vol. 12, no. 23, 2019, doi: 10.3390/en12234404.

[9] G. H. Atkinson, S. Hinmers, R. E. Critoph, and M. van der Pal, "Ammonium Chloride (NH4Cl)—Ammonia (NH3): Sorption Characteristics for Heat Pump Applications," *Energies,* vol. 14, no. 18, 2021, doi: 10.3390/en14186002.

[10] V. Goetz, F. Elie, and B. Spinner, "The structure and performance of single effect solid-gas chemical heat pumps," *Heat Recovery Systems & CHP,* vol. 13, no. 1, pp. 79-96, 1993, doi: 10.1016/0890-4332(93)90027-S.

[11] H. Bao, Z. Ma, and A. P. Roskilly, "Kinetic Models of Salt-Ammonia Chemisorption: An Overview and Comparison," in *Chemisorption: Properties, Reactions and Uses*, M. Norup Ed. United States: Nova Science Publishers, 2018.

[12] L. L. Vasiliev, D. A. Mishkinis, A. A. Antukh, A. G. Kulakov, and L. L. Vasiliev, "Resorption heat pump," *Applied Thermal Engineering,* vol. 24, no. 13, pp. 1893-1903, 2004, doi: 10.1016/j.applthermaleng.2003.12.018.

[13] C. Blackman, C. Bales, and E. Thorin, "Experimental evaluation and concept demonstration of novel modular gas driven heat pump components," presented at the 12th IEA Heat Pump Conference, Rotterdam, 18th May, 2017, O.4.7.3.